# Kinetic description of polyatomic gases with temperature-dependent specific heats

Milana Pavić-Čolić * and Srboljub Simić †
*Department of Mathematics and Informatics, Faculty of Sciences, University of Novi Sad, Trg Dositeja Obradovića 4, 21000 Novi Sad, Serbia*

(Received 4 April 2022; accepted 1 August 2022; published 17 August 2022)

In this paper we propose a Boltzmann collision operator in the continuous internal energy setting that describes polyatomic gases with temperature-dependent specific heats or thermally perfect (nonpolytropic) gases. We adopt the assumption, already presented in the Bhatnagar-Gross-Krook setup, of letting molecular internal degrees of freedom be temperature dependent and provide a method to determine its explicit dependence upon temperature from the given experimental data. We then focus on a macroscopic system of 14 moments in the nonpolytropic setting. Computation of production terms allows us to express the transport coefficients—bulk and shear viscosities and thermal conductivity—in terms of parameters from the collisional cross section. The values of these parameters are fitted to match the experimental data for Prandtl number in a certain temperature range. This led to improvement of the estimate obtained by the Eucken formula and allowed computation of the dynamic pressure relaxation time or equivalently the bulk viscosity and comparison with its estimates in the literature.

DOI: 10.1103/PhysRevFluids.7.083401

## I. INTRODUCTION

Modeling polyatomic gases at the mesoscopic scale, i.e., within the framework of kinetic theory and Boltzmann equation, is a challenging task [1]. First, one has to take into account excitation of nontranslational molecular degrees of freedom which occurs during collisions. Excitation of electrons may occur as well and contribute to the microscopic energy balance. An efficient way to model these effects is to introduce a single, continuous nonnegative variable that lumps up all the nontranslational degrees of freedom of the molecule [2–5]. So far, this approach ended up with a model in which macroscopic specific heats were constant, i.e., it yielded a model for polytropic, or calorically perfect, gases. Although conceptually simple, this way of modeling is not straightforward but comprises a variety of different models with subtleties aimed at covering diverse properties of polyatomic gases.

However, experimental evidence shows that specific heats of polyatomic gases, as well as other macroscopic properties like transport coefficients, may vary with temperature. Gases with such behavior are usually called nonpolytropic, or thermally perfect, gases [6]. Their modeling within the continuous framework of kinetic theory is an utmost challenge, since the parameters which describe the processes at mesoscopic scale should yield temperature-dependent properties at macroscopic scale. Therefore, the aim of this paper is to establish a kinetic model, based upon the Boltzmann equation with continuous internal energy state variable, describing a nonpolytropic gas.

*milana.pavic@dmi.uns.ac.rs
†ssimic@uns.ac.rs

 

The idea of the kinetic model in the continuous setting is to associate a weight function with the distribution function serving to match the proper equation of state at the macroscopic level. For the case of polytropic gases, its precise form is given in [2], which allows one to recover a linear dependence of the internal energy upon temperature (or the constant specific heat $c_v$) with a factor depending on the molecular degrees of freedom. In [3,4] the weight function is written in a general form as a function of the microscopic internal energy only, eventually enabling one to rewrite the macroscopic internal energy as a nonlinear function of temperature [7,8]. However, the specific form of such a function that matches experimentally observed behavior of the specific heat remains unknown. Recently, within the continuous approach, a more sophisticated model is provided in the Bhatnagar-Gross-Krook (BGK) setting [1,9], which encompasses rotational and vibrational modes separately by introducing two continuous internal energies and two weight functions whose form is still unknown. Finally, an abstract framework for polyatomic gas modeling is provided in [10].

Another important aspect of the continuous kinetic approach to polyatomic gases, apart from matching the specific heats, is computation of the transport coefficients, i.e., shear and bulk viscosity and thermal conductivity. To that end one has to deal not only with usual macroscopic field variables like specific energy, but also with transfer equations for higher order moments in the form of balance laws. This line of analysis is interwoven with the results of extended thermodynamics [1], which yields macroscopic equations for rarefied gases that are equivalent to moment equations of the kinetic theory. In particular, a simple asymptotic procedure, a Maxwellian iteration, relates the relaxation times of nonequilibrium macroscopic variables to the transport coefficients. Thus, it may be applied to linearized production terms computed from the collision operator to obtain explicit formulas for the viscosities and the thermal conductivity. So far, 14-moment equations with explicit linearized production terms have been established in [11,12] using the model from [4]. The physical interpretation was recently improved in [5] by considering the model [2] and the cross section proposed within the rigorous analysis in [13]. The cross sections from [12,13] contain only one free parameter used to match viscosity exponent given in [14]. A satisfactory agreement with the theoretical value of the Prandtl number given by Eucken's formula [15] with the error up to 12% is observed in [5]. This result was improved in [16] by studying the 17-moment equations and by introducing frozen collisions that do not change microscopic internal energies and consequently enriching the cross section from [13] with additional parameters. The code for computation of production terms is given in [17]. Our aim is to exploit the procedure used in the analysis of polytropic gases and apply it to the kinetic model of nonpolytropic gases that will be developed.

In this study, the kinetic model itself will be build upon ideas embodied in recently proposed BGK models [18,19], developed for temperature-dependent specific heats. In these models it was assumed that molecular degrees of freedom are temperature dependent. In our approach this amounts to letting the weight function to be temperature dependent. Using that concept we shall write the full collision operator and the Boltzmann equation by extending the work done in [2,5] to the case of nonpolytropic gases. This will allow us to study the temperature dependence of the weight function in great detail. Namely, for any given dependence of the heat capacity $c_v$ upon temperature, taken from the experimental data [20], we establish a method to explicitly determine the corresponding weight function for several polyatomic gases.

In the second step, the focus will be on the 14-moment equations, derived from the Boltzmann equation using the cross section and code for production term computation from [16,17]. By means of Maxwellian iteration [1] the models for bulk and shear viscosities and thermal conductivity or the Prandtl number will be proposed, which contain parameters coming from the cross section. For various polyatomic gases, we establish a method for the parameter fitting that finds the best possible matching with experimentally measured shear viscosity and Prandtl number in a certain temperature range. Moreover, for such a choice of parameters, we study the model for temperature-dependent bulk viscosity, a quantity hard to experimentally measure, related to the relaxation time of the dynamical pressure. We observe, as in [1,21,22], that for $CO_2$ the relaxation time of the dynamical pressure is much larger then the ones for stress tensor and heat flux at room temperature and low pressure. Moreover, the model we derive estimates that such a relation will remain on

the whole temperature range on which the shear viscosity is measured, coinciding qualitatively with [23]. The large bulk viscosity is predicted also for $H_2$ coinciding with estimates in [21] and for $CH_4$. On the other hand, as in [21], the moderate bulk viscosity is estimated for $N_2$ and CO.

Approach described above, based upon temperature-dependent weight function, is very convenient for modeling nonpolytropic gases. This statement relies on the fact that the collision operator acts only on the microscopic variables—molecular velocities and internal energies. As a consequence, all previously obtained results for the Boltzmann equation modeling polytropic gases, with the weight function depending only on the internal energy variable, can be formally extended without any change. This also includes all the macroscopic models derived from the Boltzmann equation using the moment method or the maximum entropy principle; see [1,24] and references therein.

The rest of the paper is organized as follows. In Sec. II we set up the macroscopic model of the internal energy in terms of the specific heat at the constant volume. For certain gases, we provide an explicit dependence of both specific heat and internal energy on temperature. In this section, dimensionless quantities used in the rest of the paper are defined as well. In Sec. III we establish the Boltzmann equation modeling of a nonpolytropic gas and the corresponding 14-moment model at the macroscopic level allowing to establish models for transport coefficients. In particular, we propose the weight function to be temperature dependent and provide its explicit dependence in Sec. IV by considering measurements. The rest of the section deals with parameter fitting in order to recover experimental data for the shear viscosity and the Prandtl number. The subsequent error analysis is also provided. Finally, the dynamical pressure relaxation time related to the bulk viscosity is estimated and compared with the existing results in Sec. V.

## II. MACROSCOPIC EQUATIONS OF STATE OF NONPOLYTROPIC GASES

In this paper we study thermally perfect gases which are defined as gases that obey the thermal equation of state connecting the hydrodynamic pressure $p$ with temperature $T$,

$$p = nkT, \tag{1}$$

where $n$ is the gas number density and $k$ is the Boltzmann constant, $k = 1.38 \times 10^{-23}$ J/K, and that do not necessarily have constant specific heats. This kind of gas covers variety of applications, as the condition where a gas may not be thermally perfect includes a very special combination of high pressures and low temperatures [6]. In the literature they are also known as nonpolytropic gases [19].

Temperature dependence of the specific heat at the constant volume $c_v$ (here expressed in units of kg J/K) provokes a nonlinear dependence of the specific internal energy upon temperature, written in a general form as

$$\frac{de(T)}{dT} = c_v(T), \tag{2}$$

or after integration,

$$e(T) - e_0 = \int_{T_0}^{T} c_v(\theta)\, d\theta, \quad \text{with } e_0 = e(T_0), \tag{3}$$

for some reference temperature $T_0$. We define the reference energy,

$$e_0 = T_0\, c_v(T_0), \tag{4}$$

by following [19]. We note that polytropic (or calorically perfect) gas is characterized by $c_v = \text{const}$, thus implying $e(T) = c_v T$.

In this paper we will work with dimensionless quantities. For the temperature $T \in [T_0, T_1]$ for some $T_0$, $T_1$ given, we define the corresponding scaled temperature $\hat{T}$,

$$\hat{T} = \frac{T - T_0}{T_1 - T_0} \Rightarrow \hat{T} \in [0, 1]. \tag{5}$$

Moreover, we define dimensionless heat capacity $\hat{c}_v$ and specific internal energy $\hat{e}$,

$$\hat{c}_v = \frac{m}{k} c_v, \quad \hat{e} = \frac{e}{\frac{k}{m}(T_1 - T_0)}, \tag{6}$$

where $m$ is a molecular mass in the units of kg. Using a new argument $\hat{T}$, Eq. (3) becomes

$$\frac{d\hat{e}(\hat{T})}{d\hat{T}} = \hat{c}_v(\hat{T}) \Rightarrow \hat{e}(\hat{T}) - \hat{e}_0 = \int_0^{\hat{T}} \hat{c}_v(\hat{\theta})\, d\hat{\theta}, \quad \hat{e}_0 = \hat{e}(0) = \frac{e_0}{\frac{k}{m}(T_1 - T_0)}. \tag{7}$$

Moreover, we derive $\hat{e}_0$ from (4),

$$\hat{e}_0 = \hat{c}_v(0) \frac{T_0}{T_1 - T_0}. \tag{8}$$

The exact dependence of the energy $\hat{e}$ upon temperature $\hat{T}$ can be obtained only by specifying the gas when certain experimental data can be observed. In this paper we focus on data provided by the National Institute of Standards and Technology [20] listed in the monograph [25]. In particular, we take the experimental data for the specific heat at constant pressure $c_p$ that is fitted using the Shomate equation. More precisely, Ref. [20] under "Gas phase thermochemistry data" shows the specific heat $c_p$ at the constant pressure of 1 bar in the units of J/(mol K) as a function of the temperature in K scaled by 1000, i.e., as a function of $T/1000$,

$$c_p(T) = A + B\left(\frac{T}{1000}\right) + C\left(\frac{T}{1000}\right)^2 + D\left(\frac{T}{1000}\right)^3 + E\left(\frac{T}{1000}\right)^{-2}, \tag{9}$$

with already determined explicit values of the coefficients $A$, $B$, $C$, $D$, and $E$ for each particular gas. It is then an easy task to extract, from these data, dimensionless specific heat $\hat{c}_v$ at the constant volume as a function of the scaled temperature $\hat{T}$ defined in (5),

$$\hat{c}_v(\hat{T}) = \frac{c_p[T_0 + \hat{T}(T_1 - T_0)]}{R} - 1, \tag{10}$$

where $R = 8.314$ J/(mol K) is the universal gas constant.

As an illustration of macroscopic considerations, we provide in Fig. 1 the nonlinear fit of dimensionless specific heat $\hat{c}_v$ from (9) and (10), based upon experimental data for a certain choice of gases and the temperature range

$$T \in [300, 6000]\ \text{K}, \quad \text{leading to} \quad \hat{T} = \frac{T - 300}{5700} \in [0, 1], \tag{11}$$

according to (5). It can be noticed that $\hat{c}_v$ is monotonically increasing function of $\hat{T}$, except for $Cl_2$ and $Br_2$ at high temperatures. Moreover, the temperature range in which $\hat{c}_v$ is constant, and thus corresponding to a polytropic approximation, is rather narrow and will be studied in detail in IV A 3.

## III. NONPOLYTROPIC GAS MODEL AT THE KINETIC LEVEL

### A. The Boltzmann equation

In the continuous setting, the form of the Boltzmann equation that models polytropic gases is well understood [2–4]. Its main feature is to associate a molecular velocity-internal energy pair

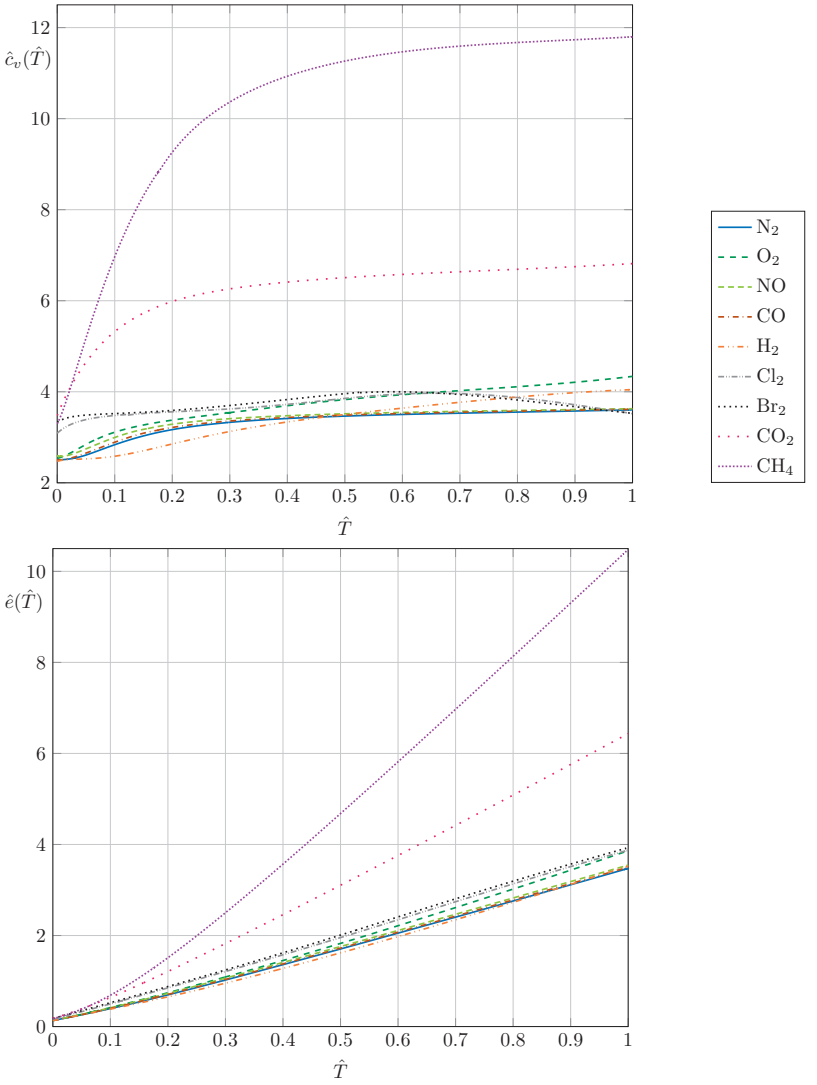


FIG. 1. The dimensionless specific heat $\hat{c}_v$ and internal energy $\hat{e}$ as functions of $\hat{T}$ from (11) for a specific choice of gas.

$(v, I)$, $v \in \mathbb{R}^3$, $I \in [0, \infty)$ to each molecule of mass $m$. Then the distribution function $f$ depends on the usual macroscopic variables, time $t \geqslant 0$, and space position $x \in \mathbb{R}^3$, and on the microscopic pair of variables $(v, I)$

$$f := f(t, x, v, I) \geqslant 0,$$

whose evolution is governed by the Boltzmann equation,

$$\partial_t f + v \cdot \nabla_x f = Q(f, f)(v, I). \tag{12}$$

The collision operator $Q(f,f)(v,I)$ describing an influence of elastic binary collisions on the change of the distribution function is given in [2] as

$$Q(f,f)(v,I) = \int_{\mathbb{R}^3\times[0,\infty)\times[0,1]^2\times S^2} \left[ f' f'_* \left( \frac{I\, I_*}{I'\, I'_*} \right)^{\alpha} - f f_* \right] \times\ \mathcal{B}(1-R) R^{\frac{1}{2}} \phi_\alpha(r)\, \psi_\alpha(R)\, d\sigma\, dr\, dR\, dI_*\, dv_*, \tag{13}$$

with standard abbreviations $f' := f(t,x,v',I')$, $f'_* := f(t,x,v'_*,I'_*)$, $f_* := f(t,x,v_*,I_*)$, where $(v',I')$ and $(v'_*,I'_*)$ are precollisional quantities, while $(v,I)$ and $(v_*,I_*)$ are postcollisional ones related through parameters of the Borgnakke-Larsen procedure [26], $\sigma \in S^2$ ($S^2$ is the unit sphere in $\mathbb{R}^3$), $r, R \in [0,1]$, and the total energy in the center-of-mass framework $E := \frac{m}{4}|v-v_*|^2 + I + I_* = \frac{m}{4}|v'-v'_*|^2 + I' + I'_*$, namely,

$$\begin{aligned} v' &= \frac{v+v_*}{2} + \sqrt{\frac{RE}{m}}\sigma, \quad v'_* = \frac{v+v_*}{2} - \sqrt{\frac{RE}{m}}\sigma, \\ I' &= r(1-R)E, \quad I'_* = (1-r)(1-R)E. \end{aligned} \tag{14}$$

The form of partition functions $\phi_\alpha(r)$ and $\psi_\alpha(R)$

$$\phi_\alpha(r) := [r(1-r)]^\alpha, \quad \psi_\alpha(R) := (1-R)^{2\alpha} \tag{15}$$

is related to the choice of the weight function,

$$\varphi(I) = I^\alpha, \tag{16}$$

where $\alpha > -1$ is a parameter of the model. In the polytropic gas case it is assumed to be constant. Scenarios for various gases that relate $\alpha$ to the number of molecular degrees of freedom and thus provide a theoretical estimate for $\alpha$ in the polytropic regime are given in [5]. In the present paper, a more sophisticated analysis based on experimental data will be given in Sec. IV A 3. Note that the form of the collision operator (13) as much as the Boltzmann model itself (12) corresponds to the *nonweighted* functional setting, as described in [5].

The cross section $\mathcal{B} := \mathcal{B}(v, v_*, I, I_*, R, r, \sigma) \geqslant 0$ is supposed to satisfy micro-reversibility conditions

$$\mathcal{B} = \mathcal{B}(v', v'_*, I', I'_*, R', r', \sigma') = \mathcal{B}(v_*, v, I_*, I, R, 1-r, -\sigma). \tag{17}$$

In this paper, we adopt the cross section model proposed in a rigorous study of the Cauchy problem for polyatomic gases in [13] and enriched with additional parameters in [16],

$$\begin{aligned} \mathcal{B}(v, v_*, I, I_*, R, r, \sigma) = K \Bigg( K_\alpha\, \omega \Bigg\{ R^{\frac{\zeta}{2}} |v-v_*|^\zeta + \eta \left[ \left( r(1-R)\frac{I}{m} \right)^{\frac{\zeta}{2}} + \left( (1-r)(1-R)\frac{I_*}{m} \right)^{\frac{\zeta}{2}} \right] \Bigg\} \\ + (1-\omega)\delta_{r-r'}\delta_{R-R'} (mE)^{-\zeta/2} \left[ \left( \frac{m}{2}|v-v_*|^2 \right)^{\zeta} + \eta_f (I^\zeta + I_*^\zeta) \right] \Bigg), \end{aligned} \tag{18}$$

where the angular part of the cross section is assumed constant, denoted by $K$, with the following physical dimensions:

$$[K] = [t] \left[ \frac{\rho}{m} \right] \left[ \frac{kT}{m} \right]^{\frac{\zeta}{2}} = \frac{\mathrm{s}}{\mathrm{m}^3} \left( \frac{\mathrm{m}^3\,\mathrm{Pa}}{\mathrm{kg}} \right)^{\frac{\zeta}{2}}. \tag{19}$$

The constant $K_\alpha$ serves to achieve consistency of the pure polyatomic collision operator with the monatomic limit as explained in [16],

$$K_\alpha = \frac{2\,\Gamma(2\alpha + 7/2)}{\sqrt{\pi}\,\Gamma(\alpha+1)^2},$$

and $\zeta > 0$, $0 \leqslant \omega \leqslant 1$, $\eta > 0$, $\eta_f > 0$ are parameters of the model. Note that $\omega$ can be interpreted as a parameter that convexly splits the pure polyatomic collision operator and the frozen one which describes collisions that do not change internal energies of particles implying $R = R'$ and $r = r'$ in (14).

Properties of the collision operator (13), such as its weak form, collision invariants, and H theorem, can be found in [2,5]. Here we will briefly summarize the conservation property of the collision operator weak form for the set of test functions $m$, $mv$, and $\frac{m}{2}|v|^2 + I$, also called collision invariants,

$$\int_{\mathbb{R}^3\times[0,\infty)} Q(f,f)(v,I) \begin{pmatrix} m \\ mv \\ \frac{m}{2}|v|^2 + I \end{pmatrix} dI\, dv = 0.$$

As a consequence, this property implies conservation laws of the mass density $\rho$, momentum density $\rho U$, and the total energy density as the sum of kinetic energy density $\frac{1}{2}\rho|U|^2$ and internal energy density $\rho e$, macroscopic quantities that can be defined as moments of the distribution function,

$$\begin{aligned} \rho &= \int_{\mathbb{R}^3\times[0,\infty)} f\, m\, dI\, dv, \\ \rho\, U &= \int_{\mathbb{R}^3\times[0,\infty)} f\, m\, v\, dI\, dv, \\ \rho\, e &= \int_{\mathbb{R}^3\times[0,\infty)} f \left(\frac{m}{2}|v-U|^2 + I\right) dI\, dv. \end{aligned} \tag{20}$$

On the other side, the entropy production is defined with the help of the test function $\log(f(v,I)I^{-\alpha})$,

$$D(f) = \int_{\mathbb{R}^3\times[0,\infty)} Q(f,f)(v,I) \log[f(v,I)I^{-\alpha}]\, dI\, dv. \tag{21}$$

The second part of the H theorem states that $D(f) = 0$ if and only if the distribution function is of the form [2,5]

$$f(v,I) = \frac{\rho}{m}\frac{1}{Z(T)}\left(\frac{m}{2\pi kT}\right)^{\frac{3}{2}} I^{\alpha}\, e^{-\frac{1}{kT}\left(\frac{m}{2}|v-U|^2 + I\right)}, \tag{22}$$

for $\rho, T > 0$, and $U \in \mathbb{R}^3$, where $Z(T)$ is a partition (normalization) function

$$Z(T) = \int_{[0,\infty)} I^{\alpha} e^{-\frac{I}{kT}} dI = (kT)^{\alpha+1}\Gamma(\alpha+1),$$

where $\Gamma$ represents the Gamma function.

The local equilibrium state can be defined by allowing $\rho$, $T$, $U$ in (22) to depend on $t$, $x$, or by formulating the maximum entropy principle as in [5], both procedures leading to the local equilibrium distribution function,

$$f_{eq}(t,x,v,I) := I^{\alpha}\frac{\rho}{m}\left(\frac{m}{2\pi kT}\right)^{\frac{3}{2}} \frac{1}{\Gamma(\alpha+1)}\frac{1}{(kT)^{\alpha+1}} e^{-\frac{1}{kT}\left(\frac{m}{2}|v-U|^2 + I\right)}, \tag{23}$$

with $\rho = \rho(t,x)$, $U = U(t,x)$, and $T = T(t,x)$. This local equilibrium distribution function (23) allows us to compute the internal energy law by following its definition (20),

$$e = \left(\alpha + \frac{5}{2}\right)\frac{k}{m}T, \tag{24}$$

for $\alpha = \text{const}$, which could be easily related to the standard form

$$e = \frac{D}{2}\frac{k}{m}T, \tag{25}$$

where $D$ is an *integer* interpreted as molecule's degrees of freedom, related to $\alpha$ as

$$D = 2\alpha + 5. \tag{26}$$

For example, in the case of (non)linear molecules with translational and rotational degrees of freedom, but without excitation of vibrational ones, we have $D = 5(6)$, which implies $\alpha = 0(1/2)$ [5]. These interpretations of the specific internal energy hold for a gas in an equilibrium state at rest at temperature $T$, when the specific heat $c_v$ is constant, $c_v = \frac{D}{2}\frac{k}{m}$, and the equipartition law is valid [19]. Although they serve as a model for polytropic gases and are assumed to be valid in nonequilibrium, departure from an equilibrium state may cause variations of $c_v$ (and consequently $D$ and $\alpha$) that sometimes cannot be ignored.

Contrary to semiclassical or discrete energy models [7,15,27–29], modeling of nonpolytropic gases is still an open question within the continuous approach. A possible extension to the case of a nonpolytropic gas starts with the idea [3,4] of finding another weight function $\varphi(I)$, different from $I^\alpha$ given in (16), which will eventually capture a nonlinear dependence of the internal energy upon temperature. This led to the moment equation hierarchy written in terms of a—still undetermined—weight function.

Another strategy, proposed in [18,19], is to let degrees of freedom be temperature dependent, i.e., to assume $D = D(T)$. In [19], such $D(T)$ is carefully called *extended* internal degrees of freedom in the nonequilibrium case, as this quantity may not be an integer anymore.

Inspired by these ideas, we build a model of nonpolytropic gases with the Boltzmann equation (12) and (13) by letting the parameter $\alpha$ depend on temperature $T(t, x)$. Since the collision operator acts only on $(v, I)$, and $(t, x)$ are seen as parameters, all previously obtained results for the Boltzmann equation in the polytropic case remain valid in the nonpolytropic case also. In particular, the local equilibrium distribution function (23) has the same functional form, except that parameter $\alpha(T)$ now also depends on $t$ and $x$ through temperature $T$. Then the internal energy density in equilibrium is of the same form as (24), and since in light of [8] the total internal energy is the same in the equilibrium and nonequilibrium, we propose the following model of the internal energy,

$$e(T) = \left(\alpha(T) + \frac{5}{2}\right)\frac{k}{m}T, \tag{27}$$

where $\alpha$ is the parameter depending on $T$. The goal of Sec. IV is to determine this parameter for a specific choice of gases by matching with experimental data.

### B. Macroscopic models for a rarefied nonpolytropic gas

Although kinetic theory provides a rather accurate description of nonequilibrium processes in gases, they are usually monitored through the behavior of macroscopic observables. We saw in Sec. III A that conserved quantities (20) are related to the local equilibrium state and the corresponding distribution function (23). Any stronger departure from equilibrium requires more information on approximate distribution function, which may lead either to the application of asymptotic methods or to the use of moment methods.

To exploit the potential of our model as much as possible, we will turn to the moment method and describe nonequilibrium processes by means of the 14-moment model. Apart from conservation laws of mass, momentum, and energy, it comprises the balance laws for the momentum flux (pressure tensor) and the energy flux (heat flux). This model turns out to be equivalent to the 14-moment model derived within the framework of extended thermodynamics [1]. In the sequel, this equivalence will provide a mean for determination of transport coefficients in terms of parameters of the kinetic model and their further use in matching the model with experimental data.

In order to accurately describe the nonequilibrium state of a polyatomic gas we need the fields of pressure tensor $p_{ij}$ and heat flux $q_i$, $i, j = 1, 2, 3$. These quantities can be defined as moments of the distribution function as well,

$$\begin{pmatrix} p_{ij} \\ q_j \end{pmatrix} = \int_{\mathbb{R}^3\times\mathbb{R}_+} \begin{pmatrix} m\, c_i\, c_j \\ \left(\frac{m}{2}|c|^2 + I\right) c_j \end{pmatrix} f\, dI\, dv, \tag{28}$$

where $c = v - U$ is the peculiar velocity. In the spirit of [8], it is important to note that the trace of pressure tensor can be related either to the nonequilibrium pressure $\mathscr{P}$ containing a dynamical pressure $\Pi$ or equivalently to the translational part of the internal energy density $\rho e_{tr}$ or translational temperature $\theta_{tr}$. More precisely,

$$\sum_{\ell=1}^{3} p_{\ell\ell} = 3\mathscr{P} = 3(p + \Pi) = 2\rho e_{tr} = 3nk\theta_{tr} = \int_{\mathbb{R}^3\times[0,\infty)} m|c|^2 f\, dI\, dv. \tag{29}$$

With this notation, the pressure tensor (28) can be written in a trace-free form,

$$p_{ij} = \sigma_{ij} + \mathscr{P}\delta_{ij}, \quad \text{with} \quad \sum_{i=1}^{3} \sigma_{ii} = 0.$$

The 14-moment macroscopic model governing evolution of the mass density, momentum density, momentum flux, energy density, and heat flux has been already derived from the Boltzmann equation in the polytropic setting [5,11]. In our notation and nonpolytropic setting it reads

$$\partial_t \rho + \sum_{j=1}^{3} \partial_{x_j}(\rho\, U_j) = 0, \quad \partial_t(\rho\, U_i) + \partial_{x_i}\mathscr{P} + \sum_{j=1}^{3} \partial_{x_j}(\rho\, U_i\, U_j + \sigma_{ij}) = 0,$$

$$\partial_t \sigma_{ij} + 2\,\mathscr{P}\frac{\partial U_{\langle j}}{\partial x_{i\rangle}} + \sum_{k=1}^{3}\left[\partial_{x_k}(U_k\sigma_{ij} + p_{\langle ij\rangle k}) + 2\sigma_{k\langle i}\frac{\partial U_{j\rangle}}{\partial x_k}\right] = P_{\langle ij\rangle},$$

$$\partial_t \mathscr{P} + \sum_{k=1}^{3}\left(U_k\partial_{x_k}\mathscr{P} + \frac{5}{3}\mathscr{P}\partial_{x_k}U_k\right) + \frac{1}{3}\sum_{k,j=1}^{3}(\partial_{x_k}p_{jjk} + 2\sigma_{kj}\partial_{x_k}U_j) = \frac{1}{3}\sum_{k=1}^{3}P_{kk},$$

$$\partial_t(\rho e) + \sum_{k=1}^{3}[\mathscr{P}\partial_{x_k}U_k + \partial_{x_k}(\rho e U_k + q_k)] + \sum_{k,j=1}^{3}\sigma_{kj}\partial_{x_k}U_j = 0,$$

$$\partial_t q_i - \left(e + \frac{\mathscr{P}}{\rho}\right)\partial_{x_i}\mathscr{P} + \sum_{k=1}^{3}\Bigg[-\left(e + \frac{\mathscr{P}}{\rho}\right)\partial_{x_k}\sigma_{ik} - \frac{\sigma_{ik}}{\rho}\partial_{x_k}\mathscr{P} + q_k\partial_{x_k}U_i + \partial_{x_k}(q_iU_k + q_{ik})$$
$$+ \sum_{j=1}^{3}\left(-\frac{1}{\rho}\sigma_{ij}\partial_{x_k}\sigma_{kj} + p_{ijk}\partial_{x_k}U_j\right)\Bigg] = Q_i, \tag{30}$$

where $A_{\langle ij\rangle}$ is the deviatoric part of the second-order tensor $A_{ij}$, defined as

$$A_{\langle ij\rangle} := \frac{A_{ij} + A_{ji}}{2} - \delta_{ij}\frac{1}{3}\sum_{\ell=1}^{3}A_{\ell\ell}.$$

Note that this system corresponds to the one from [8].

To close the system (30), we need to compute the nonconvective fluxes,

$$\begin{pmatrix} p_{ijk} \\ q_{ij} \end{pmatrix} = \int_{\mathbb{R}^3\times\mathbb{R}_+} \begin{pmatrix} m\, c_i\, c_j\, c_k \\ \left(\frac{m}{2}|c|^2 + I\right) c_i c_j \end{pmatrix} f\, dI\, dv. \tag{31}$$

To that end we will use the 14-moment approximation of the distribution function $f$, obtained in [5] via the maximum entropy principle, which yields

$$p_{ijk} = \left(\alpha + \frac{7}{2}\right)^{-1}(q_i\delta_{jk} + q_j\delta_{ki} + q_k\delta_{ij}), \quad q_{ij} = \left(\alpha + \frac{9}{2}\right)\frac{p}{\rho}\sigma_{ij} + \frac{p}{\rho}\left[\left(\alpha + \frac{9}{2}\right)\mathscr{P} - p\right]\delta_{ij}.$$

To compute production terms,

$$\begin{pmatrix} P_{ij} \\ Q_i \end{pmatrix} = \int_{\mathbb{R}^3\times\mathbb{R}_+} \begin{pmatrix} m\,c_i\,c_j \\ \left(\frac{m}{2}|c|^2 + I\right)c_i \end{pmatrix} Q(f,f)(v,I)\,dI\,dv, \tag{32}$$

apart from specifying $f$ we have to choose the cross section. In this paper, we adopt the cross section model (18), which is also used in the study of transport coefficients in the case of polytropic gases [5,16]. Therefore, for any $i, j = 1, 2, 3$, production terms (32) are computed with the help of the code available in [17]. For the sake of brevity, we will not give their explicit form here, although it can be recovered from the analysis of the next subsection.

### C. Modeling of transport coefficients using 14-moment equations

In this section we aim to determine the transport coefficients—shear and bulk viscosities and thermal conductivity—using the 14-moment model. To that end we will combine the results of previous section, i.e., production terms (32), with the results of extended thermodynamics [1]. As a first step we write the nonequilibrium pressure $\mathscr{P}$ in terms of the dynamical pressure $\Pi$ as in (29). The expression (1), together with the nonpolytropic setting (2), allows us to rewrite the derivative of internal energy density as follows:

$$d(\rho e) = (e - c_v T)d\rho + c_v\frac{m}{k}dp.$$

Using this relation, the energy conservation law (30) is equivalent to equation for hydrodynamic pressure $p$,

$$\partial_t p + \frac{(p+\Pi)}{\hat{c}_v}\sum_{k=1}^{3}\partial_{x_k}U_k + \sum_{k=1}^{3}\partial_{x_k}(pU_k) + \frac{1}{\hat{c}_v}\left(\sum_{k,j=1}^{3}\sigma_{kj}\partial_{x_k}U_j + \sum_{k=1}^{3}\partial_{x_k}q_k\right) = 0.$$

Then the equation for $\mathscr{P}$ given in (30) implies a balance law for $\Pi$,

$$\partial_t\Pi + \frac{2\hat{c}_v - 3}{3\hat{c}_v}(p+\Pi)\sum_{k=1}^{3}\partial_{x_k}U_k + \sum_{k=1}^{3}\partial_{x_k}(\Pi U_k) + \frac{2\hat{c}_v - 3}{3\hat{c}_v}\sum_{k,j=1}^{3}\sigma_{kj}\partial_{x_k}U_j$$
$$+ \frac{1}{3}\sum_{k,j=1}^{3}\partial_{x_k}p_{jjk} - \frac{1}{\hat{c}_v}\sum_{k=1}^{3}\partial_{x_k}q_k = \frac{1}{3}\sum_{k=1}^{3}P_{kk}.$$

A closure procedure of extended thermodynamics [1] shows that linearized production terms can be expressed in terms of nonconvective fluxes $\sigma_{ij}$, $\Pi$, and $q_i$ and corresponding relaxation times, $\tau_\sigma$ for stress tensor, $\tau_\Pi$ for dynamical pressure, and $\tau_q$ for heat flux [1],

$$P_{\langle ij\rangle} = -\frac{1}{\tau_\sigma}\sigma_{ij}, \quad \frac{1}{3}\sum_{k=1}^{3}P_{kk} = -\frac{1}{\tau_\Pi}\Pi, \quad Q_i = -\frac{1}{\tau_q}q_i. \tag{33}$$

On the other side, an asymptotic procedure of Maxwellian iteration recovers classical linear constitutive relations of the Navier-Stokes-Fourier model and yields relations between transport coefficients—shear viscosity $\mu$, bulk viscosity $\nu$, and thermal conductivity $\kappa$—and relaxation times

$\tau_\sigma$, $\tau_\Pi$, $\tau_q$ [1] (p. 195),

$$\mu = p\,\tau_\sigma, \quad \nu = \frac{2\hat{c}_v - 3}{3\hat{c}_v} p\,\tau_\Pi, \quad \kappa = \frac{k}{m}\,(\hat{c}_v + 1)\,p\,\tau_q. \tag{34}$$

Since linearized production terms (32) emerging from the kinetic model (12), (13), and (18) are completely equivalent to production terms (33), and the procedure described in [17] facilitates the computation of relaxation times, we can use (34) to express the transport coefficients in terms of scaled temperature $\hat{T} \in [0, 1]$ and parameters of the kinetic model. Therefore, the shear viscosity $\mu = \mu(\hat{T},\ \alpha, \zeta, \omega, \eta, \eta_f, K)$ reads

$$\mu = \frac{m}{K}\left(\frac{k}{m}(\hat{T}(T_1 - T_0) + T_0)\right)^{1-\frac{\zeta}{2}} \frac{15\,c_1}{4}[\omega c_2[15\,\eta\,k_1 + k_2\,2^{\zeta+2}(\zeta+5)] + (1-\omega)c_3[15\,\eta_f\,k_3 + k_4\,2^{\zeta+1}(2\zeta+5)]]^{-1}, \tag{35}$$

while the bulk viscosity $\nu = \nu(\hat{T},\ \alpha, \hat{c}_v, \zeta, \omega, \eta, K)$ is

$$\nu = \frac{m}{K}\left(\frac{2\hat{c}_v - 3}{3\hat{c}_v}\right)\left(\frac{k}{m}\left(\hat{T}(T_1 - T_0) + T_0\right)\right)^{1-\frac{\zeta}{2}} 3\,c_1 \frac{(\alpha+1)(4\alpha+\zeta+7)}{(2\alpha+5)} \times [\omega\,c_2[6\eta\,k_1(4\alpha+\zeta+4) + k_2\,2^{\zeta+5}(\alpha+1)]]^{-1}, \tag{36}$$

and the thermal conductivity $\kappa = \kappa(\hat{T},\ \alpha, \hat{c}_v, \zeta, \omega, \eta, \eta_f, K)$ is given by

$$\begin{aligned}\kappa = {} & \frac{(\hat{c}_v+1)\,k}{K}\left(\frac{k}{m}(\hat{T}(T_1 - T_0) + T_0)\right)^{1-\frac{\zeta}{2}} \frac{9c_1}{4}(2\alpha+7)(4\alpha+2\zeta+11)(4\alpha+\zeta+7) \\ & \times \big[\omega\,c_2(4\alpha+2\zeta+11)(\eta\,k_1\,9\{8\alpha^3 + 28\alpha^2 + 2\alpha(68-7\zeta) + (16-3\zeta)\zeta + 156 \\ & + (2\alpha+\zeta+2)[(2\alpha+\zeta+10)\zeta + (6-4\alpha)\alpha + 2]\} \\ & + k_2\,2^{\zeta+5}[12\alpha^2 + \alpha(7\zeta+57) + \zeta(\zeta+15) + 60]) \\ & + (1-\omega)4c_3(4\alpha+\zeta+7)\{3\eta_f\,k_3\{24\alpha^2 + 2\alpha(6\zeta^2 + 9\zeta + 65) + \zeta[3\zeta(\zeta+12) + 59] + 176\} \\ & + k_4\,2^{\zeta+2}[12\alpha^2 + \alpha(11\zeta+65) + \zeta(4\zeta+35) + 88]\}\big]^{-1},\end{aligned} \tag{37}$$

where constants are

$$\begin{aligned} & c_1 = \Gamma(\alpha+1)^2\,\Gamma\left(2\alpha+\zeta+\frac{11}{2}\right)\Gamma\left(\frac{4\alpha+\zeta+7}{2}\right), \quad c_2 = \Gamma\left(2\alpha+\frac{7}{2}\right)\Gamma\left(2\alpha+\zeta+\frac{11}{2}\right), \\ & c_3 = \sqrt{\pi}\,\Gamma(\alpha+1)\,\Gamma\left(\frac{4\alpha+\zeta+7}{2}\right)\Gamma\left(\frac{4\alpha+\zeta+11}{2}\right), \\ & k_1 = \pi\,\Gamma\left(\alpha+\frac{\zeta}{2}+1\right)^2, \quad k_2 = \Gamma(\alpha+1)^2\,\Gamma\left(\frac{\zeta+3}{2}\right)\Gamma\left(\frac{\zeta+5}{2}\right), \\ & k_3 = \sqrt{\pi}\,\Gamma(\alpha+\zeta+1), \quad k_4 = \Gamma(\alpha+1)\,\Gamma\left(\zeta+\frac{5}{2}\right), \end{aligned}$$

$k$ is the Boltzmann constant and $m$ molecular mass in units of kg computed as in [30], Sec. 2.10,

$$m = M_r\,u, \tag{38}$$

where $M_r$ is the relative molecular mass, a dimensionless quantity whose values can be found in [20], and $u$ is the unified atomic mass unit $u = 1.6605402 \times 10^{-27}$ kg. Parameter $\alpha(T)$ comes from the evaluation of the collision operator (13) and is modeled to be temperature dependent through its relation to the specific heat $c_v$ as will be explained in Sec. IV. Parameters of the model are $\zeta > 0$, $0 \leqslant \omega \leqslant 1$, $\eta > 0$, $\eta_f > 0$, and $K > 0$ with physical dimensions (19).

## IV. DETERMINATION OF THE MODEL PARAMETERS

In Sec. III we provided a kinetic model for nonpolytropic gases, namely,the Boltzmann equation (12) and (13) with the cross section (18). This scheme is rather general since it contains several parameters which may be adapted to provide a proper description of particular physical phenomena. The aim of this section is to propose a procedure, based upon experimental data, which determines all the parameters of the kinetic model. In particular, parameter $\alpha(T)$ will be related to specific heat $c_v(T)$ through specific internal energy, using Eqs. (2) and (27). Then, inspired by [14], parameter $\zeta$ will be related to the shear viscosity law using its experimental data; the value of the constant $K$ will be chosen in such a way to reproduce the measured value of the shear viscosity at room temperature. Finally, parameters $\omega$, $\eta$ and $\eta_f$ will be determined to obtain the best possible fit with the measured value of the Prandtl number at certain temperatures.

### A. Determination of parameter $\alpha$ from the specific internal energy

In order to solve the problem (2)–(27) for $\alpha$ using experimental data, we need to rewrite (27) in dimensionless form, by first noticing

$$\frac{e}{\frac{k}{m}T} = \alpha + \frac{5}{2},$$

and then scaling according to (6),

$$\frac{\hat{e}}{\hat{T} + \frac{T_0}{T_1 - T_0}} = \alpha + \frac{5}{2}. \tag{39}$$

Therefore, the function $\alpha(\hat{T})$ can be written in terms of an internal energy as

$$\alpha(\hat{T}) = \frac{\hat{e}(\hat{T})}{\hat{T} + \frac{T_0}{T_1 - T_0}} - \frac{5}{2}. \tag{40}$$

Finally, gathering (7) and (40) implies explicit expression of $\alpha$ in terms of the specific heat $\hat{c}_v$,

$$\alpha(\hat{T}) = -\frac{5}{2} + \left(\hat{T} + \frac{T_0}{T_1 - T_0}\right)^{-1} \left[\left(\alpha_0 + \frac{5}{2}\right)\frac{T_0}{T_1 - T_0} + \int_0^{\hat{T}} \hat{c}_v(\hat{\theta})\, d\hat{\theta}\right], \tag{41}$$

with $\alpha_0$,

$$\alpha_0 = \alpha(0) = \hat{e}_0 \frac{(T_1 - T_0)}{T_0} - \frac{5}{2} = \hat{c}_v(0) - \frac{5}{2}. \tag{42}$$

#### *1. Relation to the ratio of specific heats*

Another interpretation of the parameter $\alpha$ can be obtained by using definition of the ratio of the specific heats

$$\gamma = \frac{c_p}{c_v} = \frac{1}{c_v} + 1, \tag{43}$$

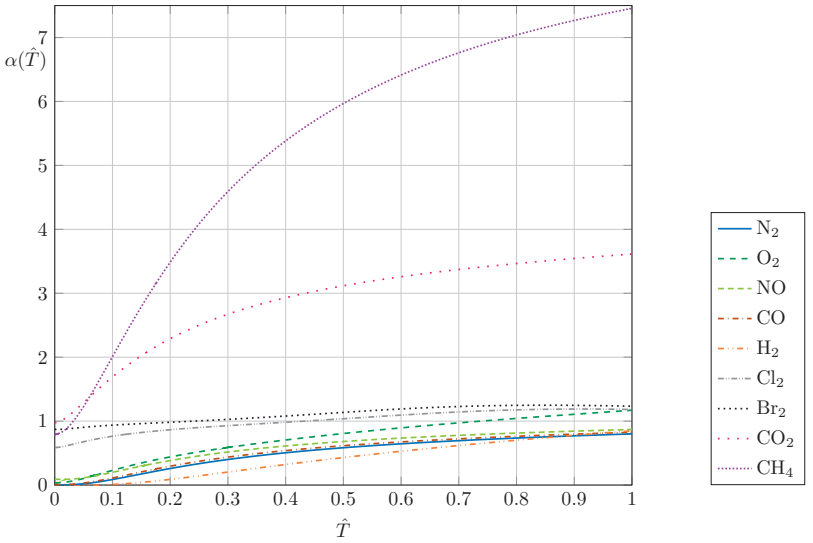


FIG. 2. Dependence of $\alpha$ upon temperature $\hat{T}$, scaled from the temperature interval [300, 6000] K.

which yields the alternative definition to (7) of the internal energy,

$$\frac{d\hat{e}(\hat{T})}{d\hat{T}} = \frac{1}{\gamma(\hat{T})-1}, \tag{44}$$

and due to this relation and differentiation of (40) with respect to $\hat{T}$ leads to

$$\gamma(\hat{T}) = \frac{\left(\hat{T}+\frac{T_0}{T_1-T_0}\right)\alpha'(\hat{T})+\alpha(\hat{T})+7/2}{\left(\hat{T}+\frac{T_0}{T_1-T_0}\right)\alpha'(\hat{T})+\alpha(\hat{T})+5/2}, \tag{45}$$

which can be reduced to the known relation $\gamma = (\alpha+7/2)/(\alpha+5/2)$ for $\alpha = \text{const}$ in the polytropic case.

#### 2. *Relation to the Eucken formula for the Prandtl number*

The Prandtl number in our notation is defined as [31]

$$\mathrm{Pr} = \hat{c}_p \frac{k}{m}\frac{\mu}{\kappa}. \tag{46}$$

It is usually estimated using the Eucken formula, written in terms of the specific heats ratio (43) as

$$\mathrm{Pr}^{(\mathrm{Eucken})} = \frac{4\gamma}{9\gamma-5}. \tag{47}$$

The relation to the parameter $\alpha$ can be obtained using (45), which reduces to $\mathrm{Pr}^{(\mathrm{Eucken})} = 2(2\alpha+7)/(4\alpha+19)$ in the case of polytropic gases [1].

#### 3. *Examples of the parameter α*

We provide in Fig. 2 examples of $\alpha(\hat{T})$ for the most common gases, such as nitrogen $N_2$, oxygen $O_2$, nitric oxide NO, carbon monoxide CO, hydrogen $H_2$, chlorine $Cl_2$, bromine $Br_2$, carbon dioxide $CO_2$, and methane $CH_4$. Our aim is to demonstrate how $\alpha(\hat{T})$ determined from the experimental data for the specific heat $c_v(T)$, provided by the National Institute of Standards and Technology [20] listed in the monograph [25], changes with temperature. Variation of $\alpha$ with $\hat{T}$ indicates

TABLE I. Behavior of $\alpha(\hat{T})$ on the scaled temperature interval [0,1] corresponding to the original temperature interval of [300, 6000] K. Values of $\alpha$ at this temperature interval endpoints are presented. We define a polytropic regime as the temperature range over which the relative change of $\hat{c}_v$ is less than 5%. As a matter of fact, the polytropic regime is around endpoints of the considered temperature range, defining two intervals: of low temperature [300, $T_l$] K scaled to [0, $\hat{T}_l$] and of high temperature [$T_h$, 6000] K scaled to [$\hat{T}_h$, 1]. For each polytropic interval, we provide the value of $\alpha$ at endpoints.

| | Temperature interval $\hat{T} \in [0, 1]$ | | Polytropic low-temperature interval $\hat{T} \in [0, \hat{T}_l]$ | | Polytropic high-temperature interval $\hat{T} \in [\hat{T}_h, 1]$ | |
|---|---|---|---|---|---|---|
| Gas | $\alpha(0)$ | $\alpha(1)$ | $T_l$ (in K) | $\alpha(\hat{T}_l)$ | $T_h$ (in K) | $\alpha(\hat{T}_h)$ |
| $N_2$ | 0.0023 | 0.8003 | 600 | 0.023 | 2670 | 0.5188 |
| $O_2$ | 0.0348 | 1.17 | 430 | 0.0511 | 4930 | 1.0505 |
| NO | 0.0901 | 0.8693 | 550 | 0.1064 | 2310 | 0.5703 |
| CO | 0.0059 | 0.8257 | 550 | 0.0241 | 2580 | 0.5388 |
| $H_2$ | −0.0301 | 0.8487 | 890 | 0.0107 | 4660 | 0.6731 |
| $Cl_2$ | 0.5869 | 1.1821 | – | | 5490 | 1.1891 |
| $Br_2$ | 0.8719 | 1.2325 | – | | 5320 | 1.2478 |
| $CO_2$ | 0.9765 | 3.6137 | – | | 2940 | 3.0544 |
| $CH_4$ | 0.7949 | 7.4567 | – | | 3040 | 5.8671 |

nonpolytropic behavior of the gas. Note that the temperature range in this section is [300, 6000] K as given in (11).

Moreover, the behavior of $\alpha$ is quantitatively studied in Table I. We first focus on the full temperature interval $T \in [300, 6000]$ K scaled to $\hat{T} \in [0, 1]$ using (11) and provide values of $\alpha$ at scaled room temperature $\hat{T} = 0$ and at $\hat{T} = 1$. One can observe that the value of $\alpha(0)$ is close to zero for $N_2$, $O_2$, NO, CO, and $H_2$, coinciding with the theoretical estimate (26) obtained for $D = 5$ that corresponds to translational and rotational degrees of freedom of a linear molecule.

Next, the focus is on the polytropic behavior of gases. We define the polytropic regime as the temperature range in which the relative change of heat capacity $\hat{c}_v$ is less than 5%, thus approximately constant. From Fig. 1, such a behavior is observed around the full temperature interval endpoints $\hat{T} = 0$ and $\hat{T} = 1$, confirming the expectations from [28]. Thus, we consider the low-temperature $T \in [300, T_l]$ K and the high-temperature interval $T \in [T_h, 6000]$ K, both scaled using (11) to $\hat{T} \in [0, \hat{T}_l]$ and $\hat{T} \in [\hat{T}_h, 1]$, respectively. In Table I temperatures $T_l$ and $T_h$ are specified, as much as values of $\alpha$ at the corresponding scaled points $\hat{T}_l$ and $\hat{T}_h$. For the low-temperature range, only $T_l > 400$ K is specified, as otherwise we cannot claim almost constant behavior of $\hat{c}_v$ over a meaningfully wide temperature range. One can notice that the polytropic behavior is experienced by gases that have, apart from translational, only rotational degrees of freedom excited at room temperature i.e., when $\alpha(0)$ close to 0. On the other side, on the high-temperature range when vibrations appear as well, all considered gases formally behave as polytropic. However, on such high temperatures a more complex modeling has to be performed. Theoretically, linear molecules for the fully excited vibrational modes are estimated to have $D = 6$ degrees of freedom corresponding to $\alpha = 1/2$ [5]. The value $\alpha(\hat{T}_h)$ suggests that this is a reasonable approximation for $N_2$, NO, and CO.

### B. Viscosity exponent $\zeta$

Inspired by [14], we will determine the parameter $\zeta$ using measurements of the shear viscosity as a function of temperature. More precisely, from [20] we use isobaric experimental data corresponding to the constant pressure $p = 1$ bar for shear viscosity on certain temperature interval $[T_0, T_1]$ K in physical units of μPa s. The first part of Table II shows the temperature interval and the observed value $\mu_0$ of the shear viscosity at temperature $T_0$ for certain gases.

TABLE II. Temperature interval $[T_0, T_1]$ K in which viscosity of a gas is measured as a function of temperature for a constant pressure $p = 1$ bar, the observed value $\mu_0$ of the viscosity in μPa s at $T_0$, and viscosity exponent $\zeta$ obtained through the fit of model function (49) with respect to the experimental data provided in [20]. Assuming $\mu = \mu_0(T/T_0)^s$, such $\zeta$ yields the value of $s = 1 - \zeta/2$ that matches the measurements. This value is compared with the one proposed in [14], Table 14, valid for the temperature range [293, 373] K.

| Gas | $T_0$ | $T_1$ | $\mu_0$ | $\zeta$ | $s = 1 - \zeta/2$ | $s$ from [14] |
|---|---|---|---|---|---|---|
| $N_2$ | 300 | 2000 | 17.89 | 0.6245 | 0.6878 | 0.738 |
| $O_2$ | 300 | 2000 | 20.652 | 0.5952 | 0.7024 | 0.773 |
| CO | 300 | 500 | 17.853 | 0.5259 | 0.7371 | 0.734 |
| $H_2$ | 300 | 1000 | 8.9385 | 0.6056 | 0.6972 | 0.668 |
| $CO_2$ | 300 | 2000 | 15.003 | 0.4008 | 0.7996 | 0.933 |
| $CH_4$ | 300 | 600 | 11.136 | 0.3806 | 0.8097 | 0.836 |

In the model for the shear viscosity (35), we first choose the value of dimensional constant $K$ whose physical dimensions are determined in (19), so that the shear viscosity at initial temperature $\hat{T} = 0$ matches the observed value $\mu_0$,

$$K = \frac{\mu(0, \alpha_0, \zeta, \omega, \eta, \eta_f, 1)}{\mu_0 \times 10^{-6}}, \tag{48}$$

where $\alpha_0$ is as in (42). For such $K$ and $\alpha_0$, the model for shear viscosity is reduced to the model function

$$\mu(\hat{T}) = \mu_0 \left[ \hat{T} \left( \frac{T_1}{T_0} - 1 \right) + 1 \right]^{1 - \frac{\zeta}{2}}, \tag{49}$$

which corresponds to the model used in [14]. Then the goal is to find the parameter $\zeta$ in order to fit the experimental data. Results are shown in Table II.

Such determined viscosity parameter $\zeta$ can be compared with the one proposed in [14]. Indeed, in [14] it is assumed that $\mu = \mu_0(T/T_0)^s$, which is the dimensional form of (49) with $s = 1 - \zeta/2$. The values of $s$ are given in [14], Table 14, valid in the temperature range [293, 373] K. The values of exponents are compared in Table II. It may be observed that there is a discrepancy between the values of exponent $s$ in the present study and [14]. Although the models are formally equivalent, computation of the exponent $s$ in our model is based upon the data in a considerably wider temperature interval than in [14], which may be considered the main cause of discrepancy.

### C. Determination of parameters $(\omega, \eta, \eta_f)$ from the Prandtl number

For the chosen $K$ as in (48), $\zeta$ from Table II, $\alpha(\hat{T})$ from (41) and $\hat{c}_v(\hat{T})$ as in (10), models for viscosity (35) and thermal conductivity (37) become functions of $\hat{T}$ that depend on parameters $\omega$, $\eta$, and $\eta_f$. The next goal is to determine these parameters in order to catch some experimental behavior of a chosen gas.

Following ideas of [16], we can determine parameters $\omega$, $\eta$, and $\eta_f$ in order to match the Prandtl number defined as (46). On one hand, as discussed in the previous paragraph, model functions of $\mu$ and $\kappa$ from (35) and (37) together with the fit for $\hat{c}_p$ as in (10), provide a model of the Prandtl number. On the other hand, using experimental data for $\hat{c}_p$, $\mu$ and $\kappa$ given in [20], we can compute the experimentally observed value of the Prandtl number at certain temperatures. Therefore, we can fit the model for the Prandtl number with respect to these data in order to find the set of parameters $\omega \in [0, 1]$, $\eta \geqslant 0$, $\eta_f \geqslant 0$ coming from the choice of the cross section (18).

We find the best possible fit for parameters $\omega$, $\eta$, and $\eta_f$ using built-in function FindFit in the *Mathematica* notebook. Results are presented in Table III, together with the maximal error of the 14-moment model for such choice of parameters. This is compared to the error of the Eucken formula

TABLE III. Parameters $\omega$, $\eta$, and $\eta_f$, with the corresponding value of $K$ from (48), chosen to fit the 14-moment model for the Prandtl number given by (46), (10), (35), and (37) with the experimental data, its maximal absolute relative error (in %), and the maximal absolute relative error (in %) of the Eucken formula introduced in (47).

| Gas | $\omega$ | $\eta$ | $\eta_f$ | $K$ from (48) | Maximal error (in %) of 14-moment model | Maximal error (in %) of Eucken formula |
|---|---|---|---|---|---|---|
| $N_2$ | 0.0056 | 88.3525 | 0.0002 | $4.2417 \times 10^{-19}$ | 4.37 | 4.98 |
| $O_2$ | 0.1217 | 1.8474 | 0.0078 | $5.3526 \times 10^{-19}$ | 1.89 | 6 |
| CO | 0.1256 | 0.7787 | 0.1782 | $9.2641 \times 10^{-19}$ | 1.2 | 1.66 |
| $H_2$ | $1.1823 \times 10^{-6}$ | 4.4763 | $7.3171 \times 10^{-6}$ | $5.5910 \times 10^{-19}$ | 3.1 | 10.31 |
| $CO_2$ | $8.4881 \times 10^{-7}$ | 0.4613 | $6.5472 \times 10^{-7}$ | $3.4604 \times 10^{-18}$ | 9.73 | 21 |
| $CH_4$ | $3.0364 \times 10^{-6}$ | 0.5395 | $5.7028 \times 10^{-6}$ | $4.3344 \times 10^{-18}$ | 5.83 | 17.21 |

introduced in (47). As a matter of fact, the error coming from the 14-moment model is lower. In addition to maximal error given in Table III, Fig. 3 shows its behavior as a function of temperature.

## V. RELAXATION TIMES

Determination of the model parameters reveals the main advantage of our procedure—we obtain a completely closed kinetic model of nonpolytropic gases (12) and (13) and (18), without undetermined parameters, and we come into position to express explicitly the relaxation times in 14-moment model once the production terms are computed through evaluation of the collision operator (13). Since the parameters are determined through matching measurable macroscopic quantities (specific heats, viscosity, and Prandtl number), relaxation times $\tau_\sigma$ and $\tau_q$ are also harmonized with experimental data. However, the importance of our results lies in the fact that we can estimate the relaxation time for the dynamic pressure $\tau_\Pi$, or equivalently the bulk viscosity $\nu$, a quantity which can hardly be measured [1].

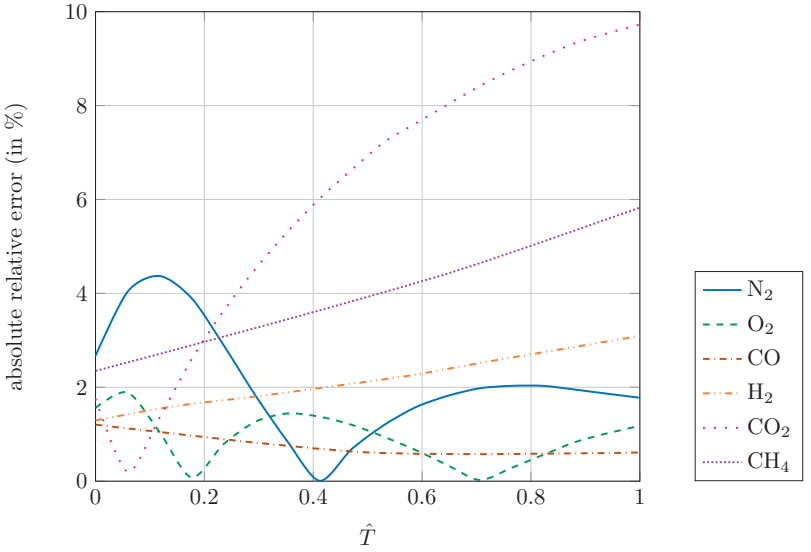


FIG. 3. The absolute relative error (in %) of the 14-moment model for the Prandtl number, (46), (10), (35), and (37) for the choice of parameters as in Tables II and III, with respect to the experimental data for certain gases.

TABLE IV. Relaxation times at $T_0 = 300$ K and $p = 69$ mmHg for certain gases as estimated by the model (35)–(37) and their relative change (50) at $T = T_1$ (or $\hat{T} = 1$) with respect to the initial state at $T = T_0$ (or $\hat{T} = 0$), with temperatures $T_1$ from Table II.

| | Values of relaxation times at $T_0$ | | | Relative change (in %) of relative relaxation times at $T_1$ with respect to $T_0$ | |
|---|---|---|---|---|---|
| Gas | $\tau_\sigma$ | $\tau_q$ | $\tau_\Pi$ | $\hat{\tau}_\sigma^*$ | $\hat{\tau}_q^*$ |
| $N_2$ | $1.9447 \times 10^{-9}$ | $2.6449 \times 10^{-9}$ | $5.6208 \times 10^{-9}$ | 10.48 | 7.64 |
| $O_2$ | $2.2449 \times 10^{-9}$ | $3.0865 \times 10^{-9}$ | $7.5744 \times 10^{-9}$ | 6.31 | 3.32 |
| CO | $1.9407 \times 10^{-9}$ | $2.6461 \times 10^{-9}$ | $9.5629 \times 10^{-9}$ | −0.02 | −0.08 |
| $H_2$ | $9.7166 \times 10^{-10}$ | $1.3999 \times 10^{-9}$ | $1.6306 \times 10^{-4}$ | 1.84 | 1.68 |
| $CO_2$ | $1.6309 \times 10^{-9}$ | $2.1946 \times 10^{-9}$ | $1.1160 \times 10^{-3}$ | 2.36 | −1.67 |
| $CH_4$ | $1.2105 \times 10^{-9}$ | $1.6325 \times 10^{-9}$ | $2.1249 \times 10^{-4}$ | 0.49 | −1.04 |

Inspired by [1], Table 8.2, we provide estimates for relaxation times $\tau_\sigma$, $\tau_q$, and $\tau_\Pi$ at temperature $T = 300$ K and pressure $p = 69$ mmHg, using models (35)–(37) and relations (34). As a matter of fact, the experimentally observed specific heat $c_p$, shear viscosity, and thermal conductivity are almost constants with respect to the pressure $p$, which allows us to use previous results obtained for $p = 1$ bar and, in particular, values of parameters given in Tables II and III. Results are presented in the first part of Table IV. As in [1,21–23], for $CO_2$ we observe that $\tau_\Pi$ is of multiple order of magnitudes greater than relaxation times $\tau_\sigma$ and $\tau_q$. Moreover, the model predicts the same behavior of $H_2$ (as also observed in [21]) and $CH_4$. On the other hand, our prediction of a moderate relaxation time $\tau_\Pi$ with respect to $\tau_\sigma$ for $N_2$ and CO coincides with estimates in [21].

The explicit expressions for relaxation times allow us to study their behavior in more detail. More precisely, we study relative relaxation times of $\tau_\sigma$ and $\tau_q$ with respect to $\tau_\Pi$, which depend solely on temperature $\hat{T}$,

$$\hat{\tau}_\sigma(\hat{T}) = \frac{\tau_\sigma}{\tau_\Pi}, \quad \hat{\tau}_q(\hat{T}) = \frac{\tau_q}{\tau_\Pi}.$$

The first part of Table IV already provides an estimate of these quantities at temperature $\hat{T} = 0$ or $T = T_0$. In addition, we can study their temperature dependence on the whole range for which viscosity is measured, that is, for $\hat{T} \in [0, 1]$ or $T \in [T_0, T_1]$, with $T_1$ from Table II. We observe that the relative relaxation times $\hat{\tau}_\sigma(\hat{T})$ and $\hat{\tau}_q(\hat{T})$ are monotonic functions of $\hat{T}$, and therefore the most extreme deviation from their state at $\hat{T} = 0$ is at state $\hat{T} = 1$. This motivates us to study the following relative change of these relaxation times:

$$\hat{\tau}_\sigma^* = \frac{\hat{\tau}_\sigma(1) - \hat{\tau}_\sigma(0)}{\hat{\tau}_\sigma(0)}, \quad \hat{\tau}_q^* = \frac{\hat{\tau}_q(1) - \hat{\tau}_q(0)}{\hat{\tau}_q(0)}. \tag{50}$$

Results are shown in the second part of Table IV. We conclude that the order of magnitudes at $\hat{T} = 0$ or $T = T_0$ for the relaxation times are preserved in the whole temperature range $\hat{T} \in [0, 1]$ or $T \in [T_0, T_1]$, with $T_1$ from Table II.

## VI. CONCLUSIONS AND OUTLOOK

In this study we proposed a closed kinetic model of nonpolytropic gases, i.e., polyatomic gases with temperature-dependent specific heats, namely, the Boltzmann equation (12) and (13) with the cross section (18). The term *closed* means that we developed a procedure for determination of the model parameters, some of which are temperature dependent and some constant, through

their accommodation to accessible experimental data. Since these data provide information about macroscopic observables, the procedure relied on an appropriate macroscopic description based upon the Boltzmann equation for polyatomic gases.

Our study was inspired by recent generalizations within the BGK kinetic framework [18,19], which assumed temperature dependence of a parameter corresponding to the molecular degrees of freedom. However, we used a kinetic description of polyatomic gases based upon a complete collision operator [2], in which the crucial role is played by a parameter $\alpha$ that facilitates matching with the specific internal energy. In the case of polytropic gases, $\alpha$ may be related to molecular degrees of freedom and assumes a constant value [2,5,16]. Following [18,19], in order to describe nonpolytropic gases, we assumed that it depends on temperature, $\alpha = \alpha(T)$. One of goals of this paper is to provide an explicit form of such parameter $\alpha(T)$ using relations between the local equilibrium distribution function and macroscopic variables to relate the parameter $\alpha(T)$ to temperature-dependent specific heats $c_v(T)$ and $c_p(T)$ by fitting the experimental data [20].

Further improvement is achieved due to a particular structure of the collision cross section (18), which contains several more parameters that may be adapted. To that end we needed a more refined macroscopic model. Thus, we decided to intertwine the 14-moment model derived from the Boltzmann equation and the corresponding 14-moment model derived in the framework of extended thermodynamics. This facilitated explicit computation of transport coefficients as functions of temperature and kinetic model parameters by using the code [17]. Experimental evidence [20] on temperature dependence of shear viscosity and heat conductivity (i.e., Prandtl number) provided a tool for determination of the cross section parameters.

Choice of the kinetic model parameters that match macroscopic observables of nonpolytropic gases also yielded a complete closure of the 14-moment model through explicit computation of the relaxation times. This is of great importance since relaxation times for the stress tensor and heat flux are harmonized with experimental data, while the bulk viscosity and relaxation time for dynamic pressure may be computed providing a reliable estimate.

Our procedure was tested on the set of polyatomic gases frequently used in literature. It turned out that our estimates improve the well-known results in [14] regarding the temperature dependence of viscosity and provide explicit expressions for the temperature-dependent bulk viscosity and relaxation time for dynamic pressure. In particular, for $CO_2$ these estimates are in a good agreement with recent studies based upon linear wave analysis [1]. Moreover, as in [21], we observe large bulk viscosity for $H_2$ and a moderate one for $N_2$ and CO.

This gives a solid basis for further applications, especially related to the moment method of kinetic theory or an equivalent description in extended thermodynamics. This combined approach has already been applied in the study of shock structure and relaxation in the multicomponent mixture of Euler fluids [32]. The procedure proposed in our study, which allows computation of the source terms for higher order moment equations for nonpolytropic gases, opens vast possibilities for analysis of nonequilibrium processes, which were rather limited so far.

More refined estimates on the bulk viscosity that are in agreement with [23] for $CO_2$ can be obtained by extending the proposed kinetic model with the total internal energy to a kinetic model that comprises rotational and vibrational internal energy separately, for example, using the idea from [9].

Moreover, it is relevant for applications to use the proposed Boltzmann equation and study the corresponding six moments model, which focuses on the dynamic pressure as the only nonequilibrium effect and is one of the rare systems that admits an exact entropy principle [5,7,33]. Parameters of the kinetic model would then allow to study various scenarios such as in the shock structure problem [22,33–35] and to compare results with other models [36].

## ACKNOWLEDGMENTS

The authors acknowledge financial support of the Ministry of Education, Science and Technological Development of the Republic of Serbia (Grant No. 451-03-68/2022-14/200125). M.P.-Č. was

supported by the Science Fund of the Republic of Serbia, PROMIS, No. 6066089, MaKiPol, as well as by holding an Alexander von Humboldt Foundation Fellowship.

[1] T. Ruggeri and M. Sugiyama, *Classical and Relativistic Rational Extended Thermodynamics of Gases* (Springer, Cham, 2021).
[2] J.-F. Bourgat, L. Desvillettes, P. Le Tallec, and B. Perthame, Microreversible collisions for polyatomic gases and Boltzmann's theorem, Eur. J. Mech. B: Fluids **13**, 237 (1994).
[3] L. Desvillettes, Sur un modèle de type Borgnakke-Larsen conduisant à des lois d'énergie non linéaires en température pour les gaz parfaits polyatomiques, Ann. Fac. Sci. Toulouse Math. **6**, 257 (1997).
[4] L. Desvillettes, R. Monaco, and F. Salvarani, A kinetic model allowing to obtain the energy law of polytropic gases in the presence of chemical reactions, Eur. J. Mech. B Fluids **24**, 219 (2005).
[5] V. Djordjić, M. Pavić-Čolić, and N. Spasojević, Polytropic gas modelling at kinetic and macroscopic levels, Kinet. Rel. Models **14**, 483 (2021).
[6] H. W. Liepmann and A. Roshko, *Elements of Gasdynamics*, Galcit Aeronautical Series(John Wiley & Sons, New York, 1957).
[7] M. Bisi, T. Ruggeri, and G. Spiga, Dynamical pressure in a polyatomic gas: Interplay between kinetic theory and extended thermodynamics, Kinet. Rel. Models **11**, 71 (2018).
[8] T. Ruggeri, Maximum entropy principle closure for 14-moment system for a non-polytropic gas, Ric. Mat. **70**, 207 (2021).
[9] T. Arima, T. Ruggeri, and M. Sugiyama, Extended thermodynamics of rarefied polyatomic gases: 15-field theory incorporating relaxation processes of molecular rotation and vibration, Entropy **20**, 301 (2018).
[10] T. Borsoni, M. Bisi, and M. Groppi, A general framework for the kinetic modelling of polyatomic gases, Commun. Math. Phys. **393**, 215 (2022).
[11] M. Pavić, T. Ruggeri, and S. Simić, Maximum entropy principle for rarefied polyatomic gases, Physica A **392**, 1302 (2013).
[12] M. Pavić-Čolić and S. Simić, Moment equations for polyatomic gases, Acta Appl. Math. **132**, 469 (2014).
[13] I. M. Gamba and M. Pavić-Čolić, On the Cauchy problem for Boltzmann equation modelling a polyatomic gas, arXiv:2005.01017.
[14] S. Chapman and T. G. Cowling, *The Mathematical Theory of Non-uniform Gases. An Account of the Kinetic Theory of Viscosity, Thermal Conduction and Diffusion in Gases*, 3rd ed. (Cambridge University Press, London, 1970).
[15] E. Nagnibeda and E. Kustova, *Non-Equilibrium Reacting Gas Flows*, Heat and Mass Transfer(Springer-Verlag, Berlin, 2009).
[16] V. Djordjić, M. Pavić-Čolić, and M. Torrilhon, Consistent, explicit and accessible Boltzmann collision operator for polyatomic gases, Phys. Rev. E **104**, 025309 (2021).
[17] V. Djordjić, M. Pavić-Čolić, and M. Torrilhon, Explicit evaluation of the polyatomic Boltzmann collision operator, github.com/Boltzmann-polyatomic/Supplements2021 (2021).
[18] B. Rahimi and H. Struchtrup, Macroscopic and kinetic modelling of rarefied polyatomic gases, J. Fluid Mech. **806**, 437 (2016).
[19] S. Kosuge, H.-W. Kuo, and K. Aoki, A kinetic model for a polyatomic gas with temperature-dependent specific heats and its application to shock-wave structure, J. Stat. Phys. **177**, 209 (2019).
[20] National Institute of Standards and Technology (NIST), U.S. Department of Commerce, NIST Chemistry WebBook, SRD 69, https://webbook.nist.gov.
[21] M. S. Cramer, Numerical estimates for the bulk viscosity of ideal gases, Phys. Fluids **24**, 066102 (2012).
[22] S. Kosuge and K. Aoki, Shock-wave structure for a polyatomic gas with large bulk viscosity, Phys. Rev. Fluids **3**, 023401 (2018).
[23] E. Kustova, M. Mekhonoshina, and A. Kosareva, Relaxation processes in carbon dioxide, Phys. Fluids **31**, 046104 (2019).

[24] M. Torrilhon, Modeling nonequilibrium gas flow based on moment equations, Annu. Rev. Fluid Mech. **48**, 429 (2016).
[25] M. J. Chase, *NIST-JANAF Themochemical Tables*, 4th ed., Journal of Physics Chemistry Reference Data, Monograph 9 in Galcit Aeronautical Series (American Chemical Society, Washington D.C., 1998).
[26] C. Borgnakke and P. S. Larsen, Statistical collision model for Monte Carlo simulation of polyatomic gas mixture, J. Comput. Phys. **18**, 405 (1975).
[27] V. Giovangigli, *Multicomponent Flow Modeling*, Modeling and Simulation in Science, Engineering and Technology(Birkhäuser, Boston, 1999).
[28] G. M. Kremer, *An Introduction to the Boltzmann Equation and Transport Processes in Gases*, Interaction of Mechanics and Mathematics (Springer, Dordrecht, 2010).
[29] M. Groppi and G. Spiga, Kinetic approach to chemical reactions and inelastic transitions in a rarefied gas, J. Math. Chem. **26**, 197 (1999).
[30] I. Mills, T. Cvitaš, K. Homann, N. Kallay, and K. Kuchitsu, *Quantities, Units and Symbols in Physical Chemistry*, 2nd ed. (International Union of Pure and Applied Chemistry, Blackwell Science, Oxford, 1993).
[31] B. E. Poling, J. M. Prausnitz, and J. P. O'Connell, *Properties of Gases and Liquids*, 5th ed. (McGraw-Hill Education, New York, 2001).
[32] D. Madjarević, M. Pavić-Čolić, and S. Simić, Shock structure and relaxation in the multi-component mixture of Euler fluids, Symmetry **13**, 955(2021).
[33] M. Pavić-Čolić, D. Madjarević, and S. Simić, Polyatomic gases with dynamic pressure: Kinetic non-linear closure and the shock structure, Int. J. Non Linear Mech. **92**, 160 (2017).
[34] S. Taniguchi, T. Arima, T. Ruggeri, and S. M., Effect of the dynamic pressure on the shock wave structure in a rarefied polyatomic gas, Phys. Fluids **26**, 016103 (2014).
[35] S. Kosuge, K. Aoki, and T. Goto, Shock wave structure in polyatomic gases: Numerical analysis using a model Boltzmann equation, AIP Conf. Proc. **1786**, 180004 (2016).
[36] D. Bruno and V. Giovangigli, Relaxation of internal temperature and volume viscosity, Phys. Fluids **23**, 093104 (2011).